Systematic evaluation of a knee exoskeleton misalignment compensation mechanism using a robotic dummy leg

Stefano Massardi[1,2], David Rodriguez-Cianca[1], Massimo Cenciarini[3], Daniel Clos Costa[3], Josep M. Font-Llagunes[3], Juan C. Moreno[1], Matteo Lancini[4] and Diego Torricelli[1]

***Abstract*— The objective and quantitative assessment of physical human-exoskeletons interaction (pHEI) represents a pressing necessity in the wearable robots field. This process remains of difficult execution, especially for early stage devices, in which the inclusion of human testing could pose ethical and safety concerns. This manuscript proposes a methodology for pHEI assessment based on an active dummy leg named Leg Replica, which is able to sense interaction forces while wearing an exoskeleton. We tested this methodology on a wearable active knee exoskeleton prototype, with the goal to evaluate the effects of a misalignment compensation mechanism. Through this methodology, it was possible to show how the misalignment compensation mechanism was able to reduce the interaction forces during passive exoskeleton motion. Such reduction was less evident when the exoskeleton was active. The tests allowed to identify specific points of improvements for the exoskeleton, enabling a more specific upgrade of the device based on these experimental results. This study demonstrates the ability of the proposed methodology to objectively benchmark different aspects of pHEI, and to accelerate the iterative development of new devices prior to human testing.**

I. INTRODUCTION

Exoskeletons have experienced an exponential growth over the past decade, and are nowadays present in multiple healthcare, industrial, and consumer contexts [1]. This rapid development led to a multitude of different products and an increasing number of prototypes that prepare for market uptake [2]. However, one problem that the community has to face is the lack of a systematic benchmarking framework to evaluate and compare these technologies. This factor is of key importance considering that a quantitative assessment is crucial for a correct inclusion of any device in the market [3]. The scientific literature includes several studies focusing on the evaluation of exoskeletons. However, the heterogeneity in protocols, metrics, and measurement systems makes it very difficult to compare the different devices to each other [4], creating a need for a systematic methodology based on standardized assessment procedures [5]. In the literature, the majority of the efforts have been centered on the assessment of performance, whereas physical interaction and safety evaluation have been less explored [6]. However, a recent survey [7] highlighted how more than half of the safety skills considered as essential requirements for rehabilitation robots were related to physical human-exoskeleton interaction (pHEI). In our opinion, one of the main problems is represented by the difficulty to directly and quantitatively assess pHEI in humans [8], [9]. Sensor placement, human variability, metrics, and protocols adopted are the main factors hampering pHEI systematic assessment [6]. Moreover, the inclusion of human subjects can often raise ethical issues, especially in early development stages, when devices generally need fast and continuous development-verification iterations. Human involvement can be partially avoided through pHEI modelling, where interaction is predicted from springs [10], spring-damper [11] or more complex digital models (DHM) [12]. However, current models still require validation with real-life measurements, while the variety and complexity of the human body remains an actual challenge. The device relative motion over the body is another important factor related to pHEI. However, the extraction of kinematic metrics is not always straightforward and is often obtained through indirect measurements [13]. This work aims to propose a new methodology for the study of pHEI based on the use of instrumented dummy limbs to improve testing repeatability and avoid human involvement in the early evaluation stages of wearable robots and new design concepts. Existing dummy-based methodologies consider wearability and device performance [14][15] while are missing of a full system for pHEI evaluation (e.g. contact force exchange). Our methodology addresses the main barriers relative to the instrumental setup for a complete pHEI measurement, as well as the necessity to conduct reproducible and systematic tests. To test the proposed methodology, we performed a pilot study focused on a well-known problem in the field of exoskeletons: joint misalignment [16]. Joint misalignment is unavoidable and responsible for undesired human-exoskeleton interaction forces. In order to limit its effect, many mechanical solutions have been proposed, e.g., misalignment compensation mechanisms [17]. These mechanisms add extra degrees of freedom (DoFs) to the exoskeleton frame to passively compensate the effects of human-exoskeleton joint misalignment and reduce spurious interaction forces. However, despite their proven theoretical advantages, the real effectiveness of misalignment compensation mechanisms remains unclear in the literature. We hypothesize that this is due to the lack of systematic and reproducible testing methods and by the difficulty introduced

[1]S.M., D.R.C., J.C.M. and D.T. are with the Neuralrehabilitation Group of Cajal Institute, CSIC, Madrid, Spain corresponding author: david.rodriguez.cianca@csic.es

[2]S.M. is with the Department of Industrial and Mechanical Engineering (DIMI), University of Brescia, Brescia, Italy

[3]M.C., D.C.C., and J.M.F.L. are with the Department of Mechanical Engineering and Research Centre for Biomedical Engineering, Universitat Politècnica de Catalunya, Barcelona, Spain

[4]M.L. is with the Department of Medical and Surgical Specialties, Radiological Sciences and Public Health (DSMC), University of Brescia, Brescia, Italy

by human tests, aggravated by the high human variability. Indeed, the evaluation of the effectiveness of these mechanisms requires direct pHEI measurements related to human-exoskeleton interaction forces and relative motions, which are not easy to measure directly in humans. This evaluation is used as test case for the dummy limb based methodology proposed by this manuscript. Our methodology is based on a robotic, sensorized replica of a human leg, called Leg Replica [18]. The leg Replica provides a standard and reproducible testbed that can be used to study multiple aspects of human-robot interaction without being affected by differences in human limb size, shape, inertia, and soft tissue characteristics. We applied the presented method to evaluate the effectiveness of a misalignment compensation mechanism implemented in a custom-made knee-joint exoskeleton under different misalignment and testing conditions. The paper is structured as follows. Section II describes the methodology adopted for this evaluation. Then, results are presented and discussed in Section III and Section IV, respectively.

II. MATERIALS AND METHODS

A. Leg-Replica prototype

The evaluation method used in this work is based on the mechatronic dummy leg called Leg Replica presented in [18]. This dummy device was designed to replicate the shape, dimensions, weight, inertia, and motion of a real human leg. The knee joint consists of an actuated hinge joint that enables position control in the sagittal plane. Hip and ankle joints are implemented as purely passive ball joints that can be locked in a predefined spatial configuration. The Leg Replica is equipped with 8 triaxial load cells located beneath its external surface, four in the thigh and four in the shank segments, (Fig. 1a). Both the thigh and shank segments include four 3D-printed surface shells made of ABS material, two at the front side and two at the back side. Each of the eight surface shells is connected via a load cell to the Leg Replica structure, allowing to sense the net interaction force applied on each surface shell. This configuration allows to obtain accurate readings of the interaction forces at the level of each physical interface (exoskeleton cuffs), while enabling high repeatability and control of the experimental conditions, which is normally difficult to achieve in human testing. An optoelectronic motion capture system composed by 8 infrared cameras (VICON, Oxford, UK) is placed around the Leg Replica platform for the estimation of the leg-exoskeleton relative displacements. A soft layer is added on the Leg Replica surface to mimic the presence of human soft tissues. Based on the recommendations provided in the ISO/TR23482-1 [19] technical report, we selected a silicon-based material (EcoFlex 00-30 Smooth-On), which demonstrated shear modulus within the range of published values for biological tissues [20]. The material was glued on both the thigh and the lower part of the shank, as visible in Fig. 1a.

B. Knee Exoskeleton prototype

For this study, we used a lightweight wearable knee exoskeleton prototype with one degree of freedom at the knee joint, developed at the BIOMEC Lab (CREB-UPC, Barcelona, Spain) (Fig 1b). The active motion is provided by the AK80-9 actuator by T-Motor which is fully back-drivable with an integrated 9:1 gear-box. The motion from the motor is transmitted to the knee joint by means of a custom cable transmission that allows bidirectional torque transmission with a 3.46:1 gear ratio to increase the nominal torque of the actuator. The shank segment of this exoskeleton features a two-rotational single-prismatic (RRP) misalignment compensation mechanism (MCM). It consists of two extra rotational joints at the exoskeleton shank frame, plus a prismatic joint that allows linear displacement of the shank cuff along the shank frame. The two-rotational component of the MCM can be deactivated to compare its effects with respect to a non-compensation condition. For this, the two extra rotational DoFs can be locked by a connecting metallic plate, while the extra prismatic joint can be locked by tightly connecting the exoskeleton shank interface to the shank frame. (Fig. 2).

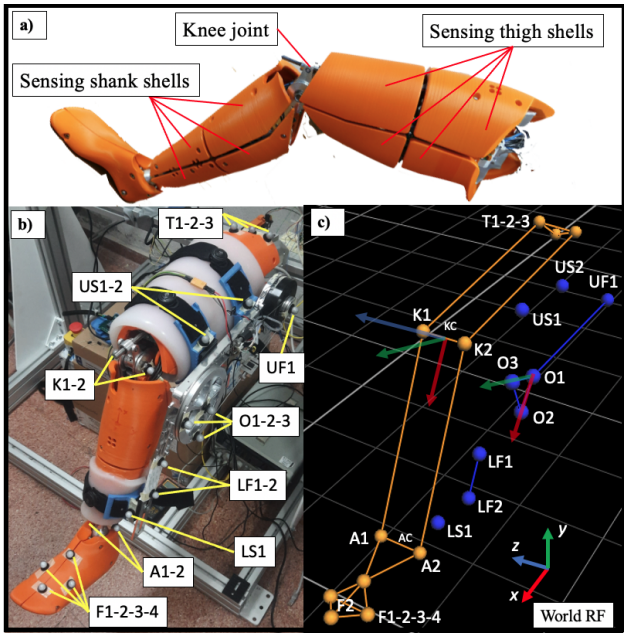

Fig. 1. (a) Lateral view of the Leg Replica prototype and its sensing surface shells. (b) Knee exoskeleton attached to the Leg Replica, including reflective markers. The implemented silicon layer to emulate soft tissue properties is visible on the thigh segment and the shank interface (white material), with the reflective markers grouped by name. (c) Leg replica's marker models, with marker labels and reference systems for the leg and knee exoskeleton. Markers were placed on the upper leg straps (US1, US2), upper exoskeleton frame (UF1), knee joint (O1, O2, O3) lower leg strap (LS1), lower exoskeleton frame (LF1, LF2), leg thigh (T1, T2, T3), leg knee hinge (K1, K2), leg ankle (A1, A2) and foot (F1, F2, F3, F4). World and local reference frames follow the following convention: x=red, y=green, z=blue

C. Experimental Protocol

In order to assess the effectiveness of the MCM to compensate for joint misalignment we explored 16 test conditions

resulting from the combination of 2 operative modes (active exoskeleton and active leg), 2 MCM configurations (OFF and ON) and for 4 misalignment conditions (neutral, positive, negative and angular), as detailed in the following (see also Fig. 3):

Operative mode

- Active exo (AE): exoskeleton driving the motion and Leg Replica set as passive.
- Active leg (AL): Leg Replica driving the motion and exoskeleton set as passive.

MCM configuration

- MCM ON: mechanism fully unlocked at both hinges and sliding component.
- MCM OFF: mechanism fully locked at both hinges and sliding component.

Misalignment condition

- Neutral misalignment: exoskeleton knee center located in a $\pm$10mm neighbor from the leg knee joint center of rotation.
- Positive misalignment: exoskeleton moved at least 30 mm along the thigh segment away from the hip joint center.
- Negative misalignment: exoskeleton moved at least 30 mm along the thigh segment towards the hip joint center.
- Angular misalignment: exoskeleton rotated about the thigh's longitudinal axis ($\approx 10^o$). As a consequence, the exoskeleton knee joint center results lower than the leg knee joint (vertical misalignment) and the joint rotation axes of the exoskeleton and the Leg Replica are not parallel with each other. An opposed and symmetric configuration to this condition was not correctly reachable, thus not included in this study.

The same angular trajectory is sent to either the Leg Replica or the exoskeleton actuator. The zero-angle reference position is set to a fully extended leg/device (leg horizontal with respect to the ground). The control trajectory is a sine-wave from 65^o (leg flexed) to 5^o (leg extended) sent at 0.1 Hz frequency. A complete run is composed of 11 sine-wave periods for each condition. The extracted metrics are described in Section II-D.

1) Marker Placement and VICON Model: To measure displacements between the exoskeleton and the Leg Replica we developed a marker-based protocol as showed in 1b. Two virtual markers for the ankle joint center (AC) and knee joint center (KC) are computed as the middle point of the segment A1A2 and K1K2, respectively. The knee reference frame (KRF) is computed with origin in KC, x-axis along KCAC, z-axis as KCK1 and y-axis as vector product of the other two. The exoskeleton knee joint reference frame (ERF) is computed with origin in O1 (placed at the center of rotation of the pulley), x-axis through marker O2 (on the pulley's circumference, in line with the shank's frame) and y-axis through O3 (on the pulley's circumference, at 90^o from O2). Segment's angles from UF1-O1 and LF1-LF2 are also computed. To avoid undesired occlusion effects, the position of markers K1 and K2 is reconstructed with respect to a fixed reference frame (RF) built from T1, T2, T3. The position of markers A1 and A2 is calculated from a fixed RF on the foot (F1, F2, F3). Markers US1 and US2 are placed to verify eventual relative motions of the thigh cuffs. Marker LS1 records both relative motions with respect to KRF (cuff rubbing) and ERF (motion enabled from the MCM unblocking).

2) Tests preparation: All trials and conditions share the same test preparation procedures. The hip of the Leg Replica is attached to a horizontal bar and blocked to maintain the thigh parallel to the ground. The Leg Replica's reflective markers are placed following the protocol described in Section II-C.1 and Fig. 1b. The leg knee joint was initially blocked at 0^o (fully extended leg) and markers' position was recorded with a VICON static capture. This preliminary step allowed to verify the residual angle between the KRF and the world reference frame (WRF). For residual angular offsets lower than 2^o, the two joint axes were considered aligned. This procedure ensures to consider the thigh parallel to the ground along the 3 axes. The ankle ball joint was locked and kept at the same predefined position for all conditions. Once the Leg Replica prototype was properly set up for the testing, the knee exoskeleton was mounted onto it. The remaining reflective markers were then placed on the exoskeleton, completing the protocol described in Fig. 1 and Section II-C.1. Before each trial, the live coordinates of markers O1 and K1 were checked to verify the alignment in the XY plane between the axes of rotation of the Leg Replica and of the exoskeleton. The cuffs were well fastened as in a real use scenario while the initial strapping forces, measured by each leg load cells, were taken as reference. For each condition, we tried to maintain the same initial strapping forces in a neighbor of $\pm$10N for each of the eight sensors in the leg. This step allows for comparing different conditions through the force metrics. Initial strapping forces were checked before each trial. After these steps, depending on the condition, a setpoint command is sent to the Leg Replica (active leg condition) or to the exoskeleton (active

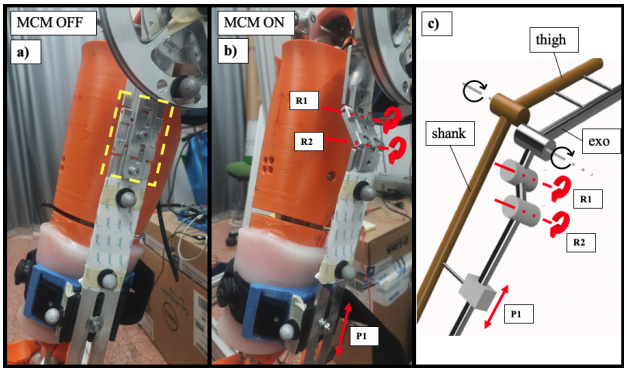

Fig. 2. Detail of the misalignment compensation mechanism when a) locked (OFF) and b) unlocked (ON). Figure c) shows the schematic coupling between the Leg-Replica and the exoskeleton, highlighting the rotational (R1, R2) and prismatic (P1) degrees of freedom.

exo condition). For each of these conditions, experiments were conducted with both the MCM ON and OFF in the different misalignment configurations, following a randomized order.

D. Metrics

The effect of the MCM was globally analyzed from total and shear forces recorded in the thigh and shank. The main metrics included in the analysis were:

- Spatial misalignment (Mx, My) [mm]: Offset in the XY plane between the axis of rotation of the Leg Replica's knee joint and that of the exoskeleton knee joint, i.e., x-y offset between the position of marker KC and marker O1 of Fig. 1b.
- Total peak force Thigh/Shank [N]: Total force was defined as the vector sum from the x-y-z components recorded by each of the 4 sensors in each segment. We considered the total force from the sum of the 4 sensors in the thigh and the 4 sensors in the shank. Total forces are then segmented on the 10 complete knee cycles of the trial (first cycle was excluded to avoid transient effects). Maximum values of each segment are collected for a total of 10 peak forces in the thigh ($F_T thigh$) and shank ($F_T shank$).
- Shear peak force Thigh/Shank [N]: The computation of this metric is analogous to that of the Total peak force. The metric only considers the force component directed longitudinally to the leg (along the x-axis of WRF for sensors in the thigh segment, and the x-axis of KRF for the sensors in the shank segment). We consider the peaks of shear forces of each sensor, recorded in the thigh segment ($F_S thigh$) and in the shank segment ($F_S shank$).
- Variation [%]: Difference in % between peaks recorded with MCM off and MCM on for the same operative mode and misalignment condition. Negative % values correspond to a force reduction after the MCM activation, positive % values to a force increase after the MCM activation.

III. RESULTS

Figure 3 shows the results obtained from the 16 tested misalignment conditions along with their position standard deviation in the XY-plane (sagittal plane). The figure shows four distinct clusters of misalignment, corresponding to positive, negative, neutral, and angular. The angular condition produced negative y-misalignments and was achieved through an extra α rotation of the exoskeleton frame about the x-axis (depicted in Fig. 3). The average rotation in the angular misalignment conditions (α) was 9.8^o. The misalignment deviation along y-axis was preponderant compared to the deviation along x-axis for both MCM ON and OFF conditions. In the MCM ON, the y-misalignment deviation was reduced in neutral (-2.1%), positive (-39.8%), negative (-75.0%), and angular (-79.1%) misalignment conditions for the active leg (AL) mode. The same effect was not clearly observed during the exoskeleton active (AE) mode where the activation of the MCM differently influenced the y-misalignment deviation in neutral (-42.9%), positive (+380%), negative (-9.7%), and angular (-4.5%) misalignment conditions.

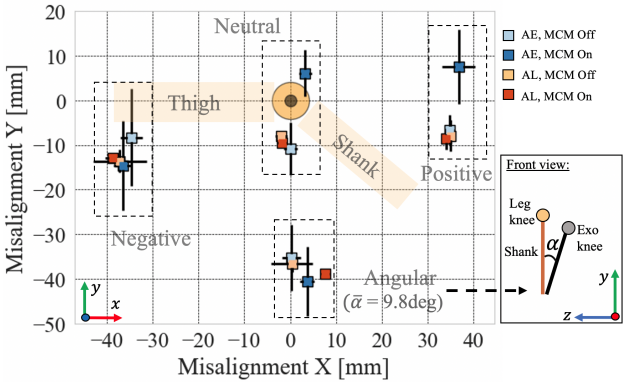

Fig. 3. XY misalignment conditions reached in the analysis. Marker coordinates represent the initial misalignment of the exoskeleton joint with respect to the leg knee joint that is here centered in (0, 0). Leg thigh and shank are shaded as pure reference to locate the misalignment (non-scaled). Markers are colored according to the operative mode and the MCM configuration. Blue markers refer to the active exoskeleton (AE) case, while red markers to the active leg (AL) case. Darker shades refer to the unlocked MCM (ON), while light shades refer to the locked MCM (OFF). The horizontal and vertical lines on each marker represents the standard deviation of the displacement of the exoskeleton knee center of rotation during the trial in the x and y directions. A depiction scheme is added to highlight the angular misalignment reference for the angular misalignment condition.

Figure 4 shows total and shear peak forces recorded in the thigh and the shank for all tested conditions. Results from the statistical difference test and percentage variation between the MCM OFF-ON conditions are included in Table I. Results are divided by operative mode, misalignment condition, and force metric considered. Results with p-value$<$0.05 are considered significantly different and marked in bold. In the AL mode, the MCM activation significantly reduced peak forces in both thigh and shank. Exceptions were found for $F_T thigh$ in positive misalignment condition and $F_S shank$ in neutral misalignment condition. All reduction effects had high significant differences, with p$<$0.001. The higher reduction effect was observed for the negative and angular misalignment conditions, with more than 30% reduction for $F_T thigh/shank$ and 50% for $F_S thigh/shank$. Shear forces showed on average higher reductions, up to 70%. In the AE mode, the MCM activation led to lower and weaker force reduction effects. More consistent effects were recorded for $F_T thigh/shank$, although 3 conditions showed no significant differences. In $F_S thigh/shank$, a force increment from 6 to 33.5% was experienced at the thigh level, while the same metric was reduced in the shank from 2.6 to 38%.

IV. DISCUSSION

In this work, we presented a pilot study where a sensorized mechatronic dummy leg was used to evaluate the effectiveness of a misalignment compensation mechanism (MCM) in a lightweight wearable knee exoskeleton prototype. The presented setup enabled to overcome typical barriers in pHEI evaluation such as the extraction of interaction forces and

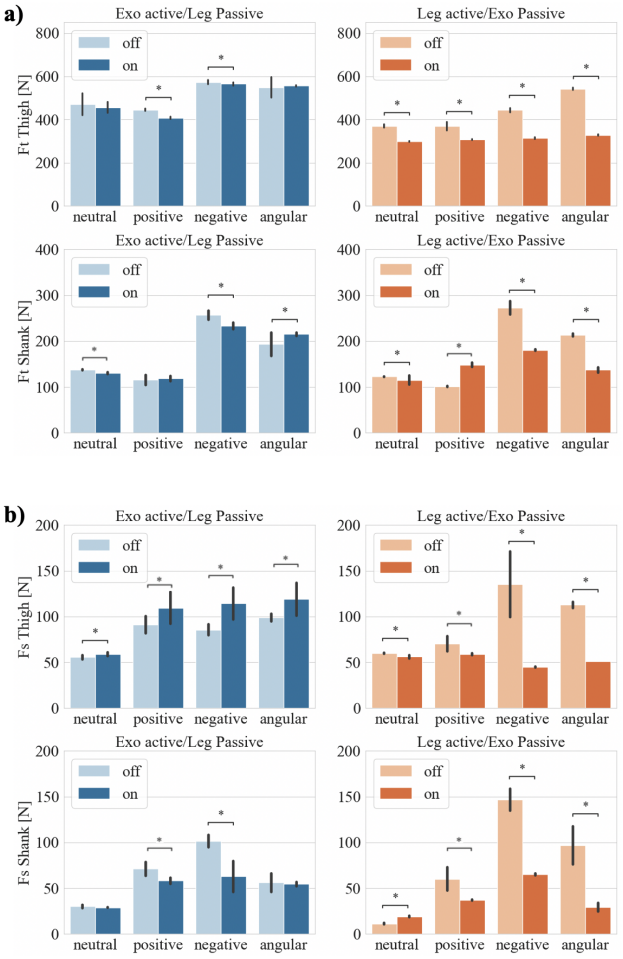

Fig. 4. Effect of the MCM on the total and shear peak forces recorded in the thigh and shank. Figure a) shows average total peak force values with its standard deviation (black error lines) in the 10 complete cycles recorded in each trial. Blue bars refer to the AE case, while orange bars to the AL case. Darker bars refer to unlocked MCM (ON), lighter bars refer to locked MCM (OFF). Significant difference between ON and OFF conditions (p-value $<$ 0.05) is marked with a * symbol. The same conventions are maintained in figure b) for shear peak force values.

TABLE I

EFFECT OF MCM ACTIVATION ON THE TOTAL AND SHEAR PEAK FORCES

	Exo Active		**Leg Active**	
	p-value	var %	p-value	var %
$F_T$thigh				
Neutral	$>$ 0.05	-3.1	$<$ **0.001**	-19.4
Positive	$<$ **0.001**	-8.5	$<$ **0.001**	-16.9
Negative	$<$ **0.05**	-1.5	$<$ **0.001**	-29.2
Angular	$>$ 0.05	+1.4	$<$ **0.001**	-39.5
$F_T$shank				
Neutral	$<$ **0.001**	-5.4	$<$ **0.05**	-6.0
Positive	$>$ 0.05	+2.6	$<$ **0.001**	+44.5
Negative	$<$ **0.001**	-9.1	$<$ **0.001**	-33.7
Angular	$<$ **0.05**	+11.3	$<$ **0.001**	-35.8
$F_S$thigh				
Neutral	$<$ **0.05**	+6.1	$<$ **0.001**	-6.6
Positive	$<$ **0.05**	+20.3	$<$ **0.001**	-16.2
Negative	$<$ **0.001**	+33.5	$<$ **0.001**	-66.8
Angular	$<$ **0.05**	+20.3	$<$ **0.001**	-54.7
$F_S$shank				
Neutral	$>$ 0.05	-3.9	$<$ **0.001**	+68.8
Positive	$<$ **0.001**	-18.5	$<$ **0.001**	-38.6
Negative	$<$ **0.001**	-38.0	$<$ **0.001**	-55.5
Angular	$<$ **0.05**	-2.6	$<$ **0.001**	-69.8

the computation of joint misalignment, normally difficult to assess systematically. The first achievement of this pilot study showed that it is possible to conduct systematic studies related to pHEI, such as the effect of MCMs to compensate human-exoskeleton misalignment, using robotic replicas of the human body, i.e., without involving humans. The second achievement was to report quantitative evidence on the effects of a MCM mechanism in different controlled and repeatable conditions. Our results showed a significant reduction of human-exoskeleton interaction forces in the presence of the MCM. This effect was significantly visible only when the Leg Replica was in active mode (exoskeleton set as passive), with few exceptions in which peak forces increased after the MCM activation. These exceptions can be the result of undesired strap loosening at the shank level, with a consequent decrease of F_Tshank and F_Sshank during the MCM OFF condition. As a result, these exceptional loosening could bias the MCM OFF-ON comparison. For the remaining conditions, the MCM considerably decreased all the force-related metrics. Regarding the AE mode, the MCM ON reduction effect was on average limited and less significant, while F_Sthigh was consistently and significantly increased when the MCM was active. The devices' backdrivability can be an important factor to consider when analyzing this discrepancy in the results. Weight, size, and transmission system, make the exoskeleton a highly backdrivable device. On the other side, the Leg Replica's backdrivability is strongly affected by its motor joint mechanical properties. We can think that more effort was requested to the exoskeleton to drive the motion. As a consequence, the knee exoskeleton was experiencing higher vertical displacements (vertical deviations in Fig 3) that the MCM activation was not able to reduce. In fact, while the Leg Replica is fixed to a stable structure, the exoskeleton frame is only fixed to the leg itself. The quality of this coupling determines how the exoskeleton will transfer its torque to the shank. From all these points, we can speculate on the possible next improvements that might regard i) the exoskeleton interfaces responsible for the exo-leg coupling, and ii) the sliding degree of freedom of the MCM (prismatic element in Fig. 2c). The rigid exoskeleton interfaces did not allow an adequate adhesion to the leg surface, influencing the system ability to correctly transfer the motor torque to the dummy. Additionally, the main limitation of the presented MCM concerns its sliding degree of freedom obtained from the nut loosening on the exoskeleton lower frame. Higher forces on this element can obstruct the correct sliding effect, thus reducing the benefits of the MCM. From these hypotheses, we can adopt a dummy-in-the-loop approach, where our improvements are first implemented and further tested and validated through our methodology. This methodology can be applied not only for the evaluation of mechanical solutions, but also to test

control strategies as well as any other implementation that could influence pHEI. One important advantage of this setup is the possibility to verify the shear component reduction. Shear forces are key metrics in pHEI evaluation, as they are normally undesired and related with rubbing effects and skin injuries. The high reduction recorded in the active leg mode confirms the advantages of implementing MCMs in exoskeletons. The possibility to test the device in AL mode produced useful data for comparison, highlighting the MCM advantages, which would not have been verified with the AE mode alone. One of the main limitations of the Leg Replica for this study is its actual degree of backdrivability. Future actions will have to quantify its ability to reproduce a passive limb behavior. Next studies will include higher number of tests and conditions to produce stronger evidence in the results. The improvements identified by this analysis will be implemented and the same methodology will be applied to the new system to test the efficacy of the improvements. This procedure can be iterated until the system will be supported with sufficient evidence before human testing, which remains an unavoidable step to prove the effectiveness of the final exoskeleton designs.

V. CONCLUSIONS

This paper proposed a dummy-based methodology to assess pHEI for the evaluation of a misalignment compensation mechanism (MCM) included in the design of a wearable knee exoskeleton. The implemented MCM proved to be effective in passive exoskeleton conditions, where the movement was driven by the dummy leg. In the active exoskeleton modality, the effectiveness of the MCM remained unclear. The tests highlighted a critical vertical displacement of the exoskeleton knee joint. The analysis identified some drawbacks of the exoskeleton interfaces and the MCM sliding mechanism, which will be the object of future improvements.

ACKNOWLEDGMENT

This work was supported by the project EXOSAFE, awarded by the COVR European Project under grant agreement No. 779966. The exoskeleton prototype used in this work was developed with funding received from the European Union's Horizon 2020 research and innovation programme under Marie Skłodowska-Curie grant agreement No. 801342 (Tecniospring INDUSTRY) and the Government of Catalonia's Agency for Business Competitiveness (ACCIÓ).

REFERENCES

[1] A. Kohli, H. Makad, N. Parekh, S. Pandey, D. Sawant, and R. Terkar, "Comparative study and analysis of lower extremity exoskeletons," in *2021 5th International Conference on Intelligent Computing and Control Systems (ICICCS)*. IEEE, 2021, pp. 889–894.

[2] V. Lajeunesse, C. Vincent, F. Routhier, E. Careau, and F. Michaud, "Exoskeletons' design and usefulness evidence according to a systematic review of lower limb exoskeletons used for functional mobility by people with spinal cord injury," *Disability and Rehabilitation: Assistive Technology*, vol. 11, no. 7, pp. 535–547, 2016.

[3] D. Torricelli, A. J. Del Ama, J. Gonzalez, J. Moreno, A. Gil, and J. L. Pons, "Benchmarking lower limb wearable robots: Emerging approaches and technologies," in *Proceedings of the 8th ACM International Conference on PErvasive Technologies Related to Assistive Environments*, 2015, pp. 1–4.

[4] D. Pinto-Fernandez, D. Torricelli, M. del Carmen Sanchez-Villamanan, F. Aller, K. Mombaur, R. Conti, N. Vitiello, J. C. Moreno, and J. L. Pons, "Performance evaluation of lower limb exoskeletons: a systematic review," *IEEE Transactions on Neural Systems and Rehabilitation Engineering*, vol. 28, no. 7, pp. 1573–1583, 2020.

[5] M. Rossini, J. Geeroms, D. Lefeber, and C. Rodriguez-Guerrero, "Automatic synthesis of arthrokinematically compatible exoskeletons. a case study on its application on a shoulder occupational exoskeleton," *Mechanism and Machine Theory*, vol. 157, p. 104186, 2021.

[6] S. Massardi, D. Rodriguez-Cianca, D. Pinto-Fernandez, J. C. Moreno, M. Lancini, and D. Torricelli, "Characterization and evaluation of human–exoskeleton interaction dynamics: A review," *Sensors (Basel, Switzerland)*, vol. 22, no. 11, 2022.

[7] J. Bessler, G. B. Prange-Lasonder, R. V. Schulte, L. Schaake, E. C. Prinsen, and J. H. Buurke, "Occurrence and type of adverse events during the use of stationary gait robots—a systematic literature review," *Frontiers in Robotics and AI*, p. 158, 2020.

[8] A. Schiele and F. C. Van der Helm, "Influence of attachment pressure and kinematic configuration on phri with wearable robots," *Applied Bionics and Biomechanics*, vol. 6, no. 2, pp. 157–173, 2009.

[9] A. H. Stienen, E. E. Hekman, F. C. Van Der Helm, and H. Van Der Kooij, "Self-aligning exoskeleton axes through decoupling of joint rotations and translations," *IEEE Transactions on Robotics*, vol. 25, no. 3, pp. 628–633, 2009.

[10] S. N. Yousaf, P. Esmatloo, K. Ghonasgi, and A. D. Deshpande, "A method for the analysis of physical human-robot interaction," in *2021 IEEE/ASME International Conference on Advanced Intelligent Mechatronics (AIM)*. IEEE, 2021, pp. 1249–1254.

[11] P. Salat Colomé, M. Jané Cardona, A. Peiret, J. M. Font-Llagunes, and M. Cenciarini, "Modelling, optimization, and simulation of a robotic assistive device for walking," in *Book of Abstracts of the XI Reunión del Capítulo Español de la Sociedad Europea de Biomecánica*, 2022, pp. 31–32.

[12] K. Bengler, C. M. Harbauer, and M. Fleischer, "Exoskeletons: A challenge for development," *Wearable Technologies*, vol. 4, p. e1, 2023.

[13] Q. Cao, J. Li, and M. Dong, "Comparative analysis of three categories of four-dofs exoskeleton mechanism based on relative movement offsets," *Industrial Robot: the international journal of robotics research and application*, vol. 49, no. 4, pp. 672–687, 2022.

[14] T. Ito, K. Ayusawa, E. Yoshida, and H. Kobayashi, "Simultaneous control framework for humanoid tracking human movement with interacting wearable assistive device," *IEEE Robotics and Automation Letters*, vol. 5, no. 2, pp. 3604–3611, 2020.

[15] W. S. Barrutia, J. Bratt, and D. P. Ferris, "A human lower limb mechanical phantom for the testing of knee exoskeletons," *IEEE Transactions on Neural Systems and Rehabilitation Engineering*, 2023.

[16] V. Bartenbach, D. Wyss, D. Seuret, and R. Riener, "A lower limb exoskeleton research platform to investigate human-robot interaction," in *2015 IEEE international conference on rehabilitation robotics (ICORR)*. IEEE, 2015, pp. 600–605.

[17] M. B. Näf, K. Junius, M. Rossini, C. Rodriguez-Guerrero, B. Vanderborght, and D. Lefeber, "Misalignment compensation for full human-exoskeleton kinematic compatibility: state of the art and evaluation," *Applied Mechanics Reviews*, vol. 70, no. 5, 2018.

[18] M. Dežman, S. Massardi, D. Pinto-Fernandez, V. Grosu, C. Rodriguez-Guerrero, J. Babič, and D. Torricelli, "A mechatronic leg replica to benchmark human–exoskeleton physical interactions," *Bioinspiration & Biomimetics*, vol. 18, no. 3, p. 036009, 2023.

[19] "ISO/TR 23482-1:2020 Robotics — Application of ISO 13482 — Part 1: Safety-related test methods," International Organization for Standardization," Technical Report, Feb. 2020.

[20] J. L. Sparks, N. A. Vavalle, K. E. Kasting, B. Long, M. L. Tanaka, P. A. Sanger, K. Schnell, and T. A. Conner-Kerr, "Use of silicone materials to simulate tissue biomechanics as related to deep tissue injury," *Advances in skin & wound care*, vol. 28, no. 2, pp. 59–68, 2015.